Vol. 576: 69–87, 2017
https://doi.org/10.3354/meps12233

MARINE ECOLOGY PROGRESS SERIES
Mar Ecol Prog Ser

Published August 3

Evolution of long larval life in the Australasian rock lobster *Jasus edwardsii*

Stephen M. Chiswell[1,*], John D. Booth[2]

[1]National Institute of Water and Atmospheric Research, Wellington 6021, New Zealand
[2]488 Rawhiti Rd, Bay of Islands 0184, New Zealand

ABSTRACT: The Australasian red (southern) rock lobster, *Jasus edwardsii* (Hutton, 1875), has a pelagic larval duration (PLD) of 18–20 mo, which may be the longest PLD of any crustacean. This PLD compares with 8–12 mo for 2 other species of rock lobster that occupy overlapping latitudinal ranges in Australia and New Zealand, *Sagmariasus verreauxi* and *Panulirus cygnus*. In this article, we examine 2 hypotheses using a Lagrangian individual-based bio-physical model (IBBM). The first hypothesis is that the long PLD of *J. edwardsii* occurs simply because it is a cool-water species, and its larvae require longer to develop in the cool ocean temperatures around southern Australia and New Zealand. The second hypothesis is that the long PLD of *J. edwardsii* evolved because some feature in the ocean circulation around Australia and New Zealand led to selection for longer larval duration. We find that potential settlement around Australia shows strong annual cycles with higher settlement in winter, probably caused by stronger onshore Ekman flow in winter. For larvae hatching in spring, those that can delay metamorphosis for 20–21 mo after hatching can take advantage of this higher potential settlement and thereby increase recruitment. Although we cannot exclude temperature as a factor in the evolution of long PLD, we suggest that the long PLD of *J. edwardsii* may well be an evolutionary response to these strong annual cycles of oceanic circulation that impact potential settlement.

KEY WORDS: Evolution · Larval duration · Numerical simulation · Rock lobster

INTRODUCTION

The Australasian red (southern) rock lobster, *Jasus edwardsii* (Hutton, 1875), which supports large fisheries in coastal waters around New Zealand and southern Australia, has a pelagic larval duration (PLD) of at least 12 mo, and possibly as long as 24 mo (Booth 1994). This PLD has often been stated as likely to be the longest larval duration of any crustacean (e.g. Pollock 1995) and may be the longest PLD of any benthic animal, with data from New Zealand and Australia showing settlement peaking about 18–20 mo after hatching (Chiswell & Booth 2008, Bradford et al. 2015).

Jasus is a pan-Southern Hemisphere genus of rock lobsters (Palinuridae) found mainly between 27° and 45° S, which is thought to have radiated from a predecessor of the extant deep-water genus *Projasus* 5 to 25 million years ago following the opening of the Drake Passage (Pollock 1995). With the exception of *J. edwardsii* and *J. lalandii*, which are found around southern Africa, the other members of *Jasus* are endemic to isolated island/seamount groups (Booth 2006) and mostly have unknown PLDs. *J. frontalis* is found solely around Juan Fernandez and Desventuradas Islands in the south-eastern Pacific Ocean. *J. caveorum* is known only from a single seamount chain about 4500 km west of these islands. *J. paulensis* is found around Île Saint-Paul and Amsterdam Island in the southern Indian Ocean, and *J. tristani* is found around Tristan da Cunha and Gough Islands and the Vema Seamount in the southern Atlantic Ocean (although Groeneveld et al. 2012 suggest that *J. paulensis* and *J. tristani* should be synonymized as *J. paulensis*).

*Corresponding author: s.chiswell@niwa.cri.nz

The long PLD of *J. edwardsii* suggests that either long PLD is a feature of *Jasus* species in general, or that it evolved specifically in *J. edwardsii*. Other estimates of PLD for this genus are about 12 mo for *J. frontalis* (Porobi et al. 2013 and references therein) and 9–10 or 14–18 mo for *J. lalandii* (Pollock 1986, George 2005 and references therein). These estimates point to a long PLD evolving specifically in *J. edwardsii*, but they are too uncertain to be definite that this is the case.

Having a PLD that is too long may be counterproductive for isolated island populations, because it reduces the chances of local settlement of larvae. Since dispersal distance generally scales with PLD (e.g. Siegel et al. 2003), in the absence of other factors one would assume that populations living on isolated islands would select for shorter PLDs. This supports the idea that long PLD evolved specifically for *J. edwardsii* living on the large land masses of Australia and New Zealand. If so, the long PLD of *J. edwardsii* may have been selected for by some feature of the ocean circulation around Australia and New Zealand. Such a feature might be an offshore eddy that entrains larvae and eventually brings them back close to the coast some time later, similar to the Wairarapa Eddy which is thought to be effective in retaining larvae off New Zealand (Chiswell & Booth 1999).

Two other species of rock lobster, *Sagmariasus verreauxi* and *Panulirus cygnus*, occupy overlapping latitudinal ranges in Australia and New Zealand, but have PLDs of between 8 and 12 mo — markedly shorter than that of *J. edwardsii* (see Table 1). *S. verreauxi* and *P. cygnus* are found generally to the north of *J. edwardsii* in warmer coastal waters on the eastern and western coasts of Australia, respectively. *S. verreauxi* is also found in northeast New Zealand (Booth 2011). It has often been noted that larval development in warm waters is faster than in cold waters (e.g. O'Connor et al. 2007, Oliphant et al. 2013) and it may simply be that the longer PLD of *J. edwardsii* reflects the fact that this species occurs in cooler water. Yet it is the oceanic temperatures experienced by larvae during their pelagic phase, not the coastal temperature where adults live, that affects larval development. With an 8–12 mo PLD, larvae can potentially disperse widely and it is not clear *a priori* that the oceanic temperature experienced by *S. verreauxi* and *P. cygnus* larvae during their pelagic phase is markedly different from that experienced by *J. edwardsii* larvae.

In this article, we examine 2 alternative hypotheses concerning the PLD of the Australasian rock lobster. The first hypothesis is that the long PLD reflects the fact that *J. edwardsii* is a cool-water species, and its larvae experience cooler ocean temperatures than do the other *Jasus* species. The second hypothesis is that the long PLD of *J. edwardsii* is selected for by some feature in the ocean circulation around Australia and New Zealand. We use an individual-based bio-physical model (IBBM), where the dispersal of larvae was simulated using a data-assimilating eddy-resolving ocean circulation model of the circulation around Australia and New Zealand. The hydrodynamical model, described in detail later, is a high resolution hindcast of the ocean circulation from 1993 to 2012.

Two sets of simulations are presented here. The first set, which we denote as the generalised simulation, was designed to investigate how spatial and temporal kernels of settlement depend on PLD for locations around Australia and New Zealand without regard to present-day populations. By making no assumptions about present-day adult distributions or settlement, this exercise was designed to investigate both how the temperature experienced by larvae during dispersal relates to the coastal temperature at settlement, and whether there are regions where ocean circulation alone leads to a particular PLD being favoured.

As well as these generalised simulations, we examine species-specific simulations where hatching occurs only at present-day adult distributions. These species-specific simulations were designed to model present-day larval dispersal for the 3 species of interest. They were intended both to confirm that the particle-based simulations adequately mimicked present-day larval dispersal, and to investigate the 2 hypotheses under consideration.

This article is laid out as follows. After short summaries of the ocean circulation around Australia and New Zealand and of the lifecycles of the 3 lobster species, we describe the hydrodynamical hindcast and the particle-based methods. In the 'Results' section, we describe first the results of the generalised simulation, then of the species-specific simulations. Finally we present our summary and discussion.

Ocean circulation around Australia and New Zealand

Mean sea surface temperature in the region ranges from 10°C in the south of New Zealand to 28°C in the north of Australia (World Ocean Atlas climatology; Locarnini et al. 2010) (see Fig. 1). Australia is unique

among the continents in that the boundary currents on both the west and east coasts flow poleward. The dominant current off the west coast is the Leeuwin Current, which flows south along the west coast then eastwards close inshore south of Australia, where it is also known as the South Australian Current (Godfrey & Ridgway 1985, Feng et al. 2003). South and offshore from the South Australian Current, the Flinders Current flows westward (Middleton & Cirano 2002). Off the east coast, north of 20°S, the North Queensland Current flows equatorward (Kessler & Gourdeau 2007), south of 20°S, the East Australian Current and its extension (Boland & Church 1981) flows poleward to about Bass Strait. Much of the flow in the East Australian Current then recirculates and flows across the Tasman Sea as the Tasman Front. The Tasman Front attaches to the east coast of New Zealand as the East Auckland Current (Stanton et al. 1997), part of which then flows into the East Cape Current (Chiswell et al. 2015 and references therein). In the south of New Zealand, the Southland Current flows north-eastward along the east coast of the South Island (Heath 1972).

Lobster lifecycles

Adults of all 3 Australasian rock lobster species are found in depths up to ~100 m along the coast. Egg hatching occurs between September and February depending on the species. The larval form of these species is called a phyllosoma, which spends its time offshore moulting many times before metamorphosing into the short-lived, non-feeding, post-larval puerulus which then swims inshore to settle. The puerulus then moults into the first-instar juvenile (Booth 2002). Estimates of PLD are made from the difference in timing between egg hatching and puerulus settlement at the same location, and show a wide range, usually attributed to the spread in time of both hatching and settlement. However, the PLD estimates can be in error if the settlement occurs from distant hatching, and that distant hatching occurs at a different time to the local hatching.

J. edwardsii are found from southern Western Australia around Tasmania to central New South Wales, although they are most abundant between central South Australia and Tasmania. They are also found on seamounts in the Tasman Sea and in all mainland New Zealand waters, but the main New Zealand populations are on the east coast of the North Island, around Stewart Island, in Fiordland and at the Chatham Islands (Booth 2006 and references therein). Settling densities, estimated in part from puerulus collectors, do not exactly mirror the adult populations, with adults found upstream of the main settling regions (see Fig. 2). This mismatch is maintained by the contranatant migration of juveniles (Booth 1997). *J. edwardsii* larvae hatch in spring between September and November. Settlement data from puerulus collectors show settlement is spread over several months, with considerable interannual variability in magnitude and timing, but on average, peak settlement is in July in South Australia (Linnane et al. 2010) and in June in New Zealand (Chiswell & Booth 2008).

P. cygnus are found in Western Australia, between Cape Leeuwin and North West Cape (see Fig. 3), with highest abundance between Geraldton and Perth (Fletcher et al. 2005). Phyllosomas hatch in summer from November to February (Griffin et al. 2001) with puerulus settlement peaking between September and January, depending on location (de Lestang et al. 2012). There is a documented northward contranatant migration by young juvenile 'whites' from nurseries into breeding grounds (de Lestang & Caputi 2015).

S. verreauxi are mostly found in New South Wales and the northeast coast of the North Island of New Zealand, although isolated individuals can be found as far south as Tasmania and around the west and south coasts of the South Island of New Zealand (Fig. 3). *S. verreauxi* larvae hatch in summer in December and January, and they are thought to have an 8–12 mo PLD (Montgomery & Craig 2005, Booth 2011). In both Australia and New Zealand, strong boundary currents (East Australian, East Auckland and East Cape Currents, respectively) cause puerulus settlement to occur downstream of the adult populations, and this species is known to have a strong contranatant migration of juveniles (Booth 2011).

For all 3 species, there is some diel vertical migration in phyllosomas, where they sink during the day to avoid predation and return to the near-surface at night to feed (e.g. Bradford et al. 2005). Griffin et al. (2001) showed that for *P. cygnus* such vertical migration is critical in maintaining larval retention off Western Australia, where the deep currents can be in opposite directions to the near-surface currents. Actual diel migration profiles are difficult to ascertain and probably depend on the phyllosomas' developmental stage (Bradford et al. 2005, Butler et al. 2011, Feng et al. 2011 and references therein).

It is well established that the puerulus is a non-feeding stage, and that the swim to the coast is made on stored energy (Jeffs et al. 2001). Therefore, for

successful settlement, metamorphosis needs to take place closer to the coast than the swimming range of the puerulus. There is debate about the triggers for metamorphosis, where metamorphosis takes place, and how larvae navigate to coast (e.g. Jeffs et al. 2005, Hinojosa et al. 2016). Jeffs et al. (2001) found newly metamorphosed *J. edwardsii* pueruli from New Zealand up to 200 km offshore with a median distance offshore of 92 km. Most likely, the maximum swimming range for pueruli depends on the species, but here we assume that the maximum range of pueruli is 100 km.

METHODS

Bluelink hindcast

Ocean currents for the simulations were obtained from the Bluelink ReANalysis 3.5 (hereafter, Bran 3.5) hindcast of currents around Australian and New Zealand. The methodology behind Bran 3.5 is described comprehensively in Oke et al. (2013), and is based on a *z*-level primitive equation ocean model with no explicit horizontal diffusion. The model assimilates data including sea-surface height and temperature derived from satellites, and temperature and salinity profiles from Argo floats.

Bran 3.5 has 1/10° resolution around Australia and New Zealand, but extends to coarser resolution west of 90°E and east of 180°E to give near-global coverage. Bran 3.5 covers the 19.5 yr from 1 January 1993 to 31 July 2012. It is initialised to a blend of climatologies and is driven at the surface by fluxes of momentum, heat and freshwater from reanalysed fields. Thus, Bran 3.5 is intended to provide a best estimate of the ocean currents in the Australia–New Zealand region from 1993 to 2012. It does not include tides or wind waves, and in particular the Stokes drift is not explicitly modelled.

Bran 3.5 has 51 levels in the vertical. We extracted daily-mean velocity fields from model depths of 12.5 and 100.5 m to provide surface and deep current fields in the simulations. The 12.5 m depth was chosen rather than the 2.5 m level because the 2.5 m level is thought to have too-strong Ekman flows (P. Oke pers. comm.). In addition, the 12.5 m level has been validated against observed near-surface drifter velocities (Chiswell & Rickard 2014).

The evolution of long PLD in *Jasus edwardsii* most likely occurred over the last 2 to 5 million years since the radiation of the proto *Jasus* genus, and undoubtedly the ocean circulation has changed over that time, so that ideally this analysis should be made with paleo-ocean models. But suitable paleo-ocean models do not exist. Thus, the strict interpretation of this work is that the findings reflect the present-day evolutionary selection, if any, in the region. Since evolution of long PLD is likely to have occurred over thousands or millions of years, we infer that if present-day ocean circulation selects for long PLD, then it is reasonable to assume that the present-day ocean is at least broadly representative of the paleo-ocean.

Simulations, settlement and adult distributions indices

In the single-particle method (e.g. Chiswell & Rickard 2008), trajectories are calculated for individual particles released at regular intervals from a source location. The resulting ensemble of trajectories is assumed to represent the likely dispersal from that location, e.g. the spatial kernel for a PLD of 18 mo is represented by the distribution of simulated particles 18 mo after release.

For the generalised simulation, 103 hatching locations spaced about 100 km apart were chosen around Australia and New Zealand south of 15°S (Fig. 1). The 15°S limit was chosen because north of this latitude larvae are likely to be dispersed by the North Queensland Current (NQC; Kessler & Gourdeau 2007), and also, this latitude is well north of the distributions of the 3 species investigated here. Six geographic regions were defined as Western, Southern and Eastern Australia and North, South and Chatham Islands of New Zealand, denoted as WA, SA, EA, NI, SI and CI, respectively (Fig. 1). The WA–SA and EA–SA boundaries were chosen to be at about the southern limits of *Panulirus cygnus* and *Sagmariasus verreauxi* distributions, near Capes Leeuwin and Howe in the west and east, respectively.

Because Bran 3.5 is an open-ocean hindcast and does not necessarily model the coastal or wind-driven circulation that takes larvae from their hatching near the coast into the open ocean, these hatching locations were placed 60 km from the coast (i.e. we made the assumption that larval transport from hatching near the coast to 60 km offshore occurs quickly in comparison to the PLD). The coast is quite complicated, and some locations got pushed offshore by promontories or islands, e.g. by Barrow island off central WA.

Trajectories were computed using a 4th order Runge-Kutta advection scheme with no added diffu-

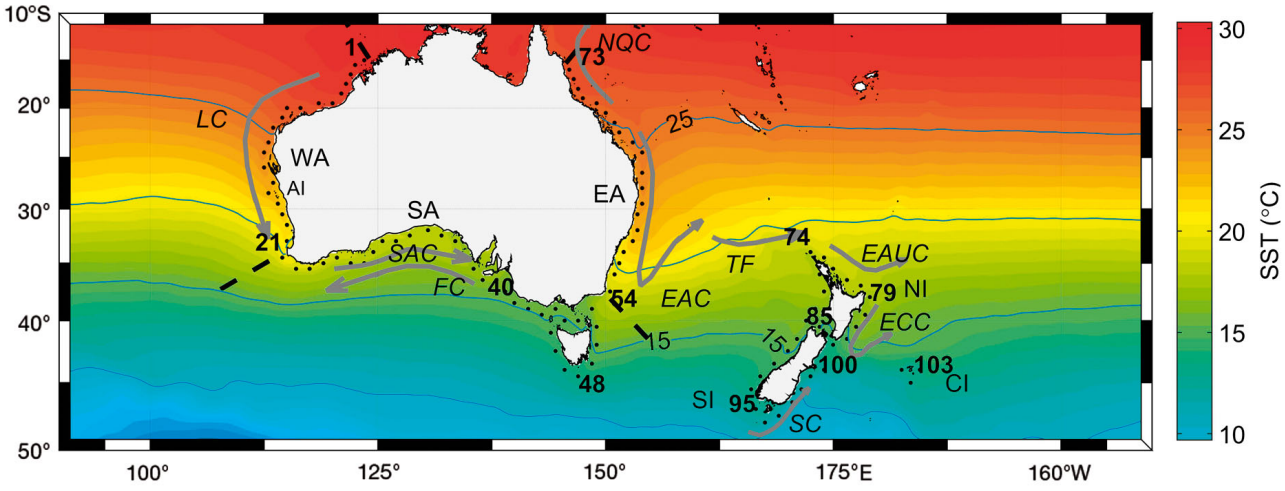

Fig. 1. The 103 hatching locations (black dots) used in numerical simulations superimposed on mean sea surface temperature (SST). Locations were spaced ~60 km offshore and ~100 km apart around Australia and New Zealand, and were classified into 6 regions corresponding to Western, Southern, Eastern Australia (WA, SA, EA), and the North, South and Chatham Islands of New Zealand (NI, SI, CI). Bold numbers (1, 21…103) indicate the index number of the hatching locations. The Albrolhos Islands (AI) are off the coast of WA. Major currents shown schematically are: LC: Leeuwin Current; SAC: South Australian Current; FC: Flinders Current; NQC: North Queensland Current; EAC: East Australian Current; TF: Tasman Front; EAUC: East Auckland Current; ECC: East Cape Current; and SC: Southland Current (Chiswell et al. 2015)

sion. Trajectories were computed using a 1 d time step, which is too short to resolve any diel migration. Thus, based on the pattern used by Griffin et al. (2001), where phyllosomas spend 2/3 of their time at the surface and 1/3 of their time at 100 m, the trajectories were computed using weighted averaged currents from the 2 levels (i.e. 2/3 of velocity at 12.5 m, and 1/3 of velocity at 100.5 m).

We released larvae at each hatching location on the first day of every month for 16 yr, from 1 January 1993 to 1 December 2008, and computed their trajectories for 36 mo, allowing us to consider PLDs up to 36 mo. Thus, there were 192 trajectories from each hatching location. Trajectories could have been computed at more frequent intervals, but since the velocity Eulerian timescale is about 1 mo (Chiswell 2013), these trajectories would not be independent.

We did not explicitly model metamorphosis or the mechanisms determining puerulus navigation. Instead, to compute potential settlement for a given PLD, we assumed that there is a 30 d competency period for metamorphosis centred on that PLD. We also assumed that pueruli have a maximum swimming range of 100 km (based on Jeffs et al. 2001), and that any simulated larvae that are within this distance of the coast during the competency period will settle. Thus the potential settlement has units of number of settlers per 30 d.

For example, for 6 mo PLD, the competency period is from 168 to 197 d after hatching. Each trajectory was inspected to see if it passed within the 100 km settlement zone during this time, and potential settlement was computed based on the amount of time the simulated larvae spent in the settlement zone. If a simulated larva spent 10 d during the competency period in the settlement zone it counted as 10 settlers, whereas if it only spent 1 d in the settlement zone it counted as 1 settler. This algorithm allows for the fact that in reality a phyllosoma spending 10 d in the settlement zone is much more likely to metamorphose into a puerulus and settle than a phyllosoma that momentarily crosses into the zone. For the purpose of calculating the statistics, settlement was binned into 103 geographic bins corresponding to the 103 hatching locations.

The 30 d competency period was based on the width of the observed settlement peaks in Australia, and this, along with the 100 km swimming distance were somewhat subjective choices. However, sensitivity studies (results not shown) indicated that increasing or decreasing these parameters by up to a factor of 2 did not materially affect where settlement occurred, although the number of settlers was approximately proportional to both these parameters.

Once each trajectory was computed, the mean temperature experienced by each simulated larva during its pelagic phase, denoted mean temperature during dispersion (MTD), was computed using mean ocean temperature from the World Ocean Atlas climatology (Locarnini et al. 2010). To account for diel

vertical migration, the ocean temperature was weighted as 2/3 of the sea surface temperature and 1/3 of the temperature at 100 m.

For the species-specific simulations, we selected the subset of the generalised simulation trajectories that had the appropriate hatching locations and months for that species. For example, for *J. edwardsii* simulations, we selected trajectories from the generalised simulation that originated in *J. edwardsii* adult population areas and were hatched between September and November. In the absence of sufficiently detailed spatial distribution hatching and settlement, we assigned hatching and settlement in terms of absence/presence at each of the 103 hatching locations. These distributions are shown in Figs. 2 & 3, and are estimates of the distribution of 90% of adults and settlers around Australia and New Zealand based on available data from a number of sources (Annala et al. 1980, Brown & Phillips 1994, Montgomery & Craig 2005, Chiswell & Booth 2008, Booth 2011).

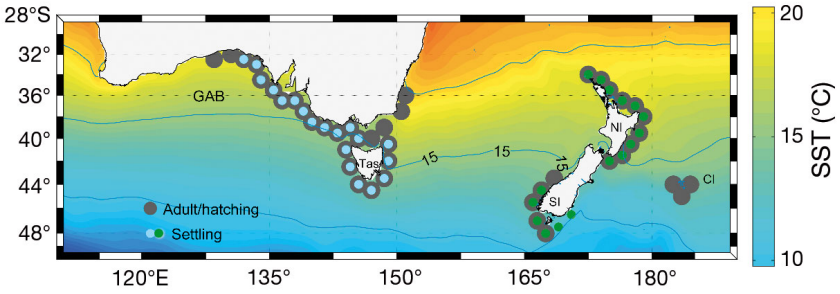

Fig. 2. Adult/breeding populations and puerulus settling distributions used in simulations of *Jasus edwardsii* larval dispersal, based on compilation of observations (Annala et al. 1980, Brown & Phillips 1994, Chiswell & Booth 2008). Grey dots: adult/breeding stock locations; cyan and green dots: settling locations in Australia and New Zealand, respectively. GAB: Great Australian Bight; Tas: Tasmania; SI: South Island; NI: North Island; CI: Chatham Islands

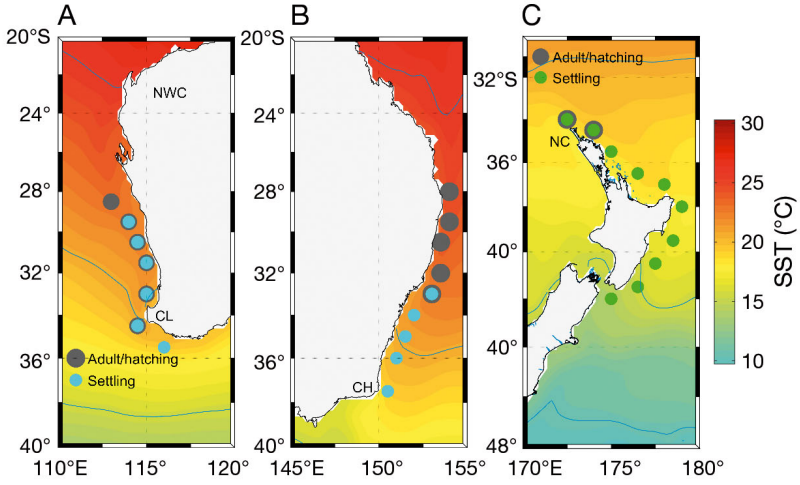

Fig. 3. Adult/breeding populations and puerulus settling distributions used in simulations of larval dispersal. Grey dots: adult/breeding stock locations; cyan and green dots: settling locations in Australia and New Zealand, respectively. (A) *Panulirus cygnus* based on compilation of observations (Brown & Phillips 1994). NWC: Northwest Cape; CL: Cape Leeuwin. (B,C) *Sagmariasus verreauxi* based on compilation of observations (Brown & Phillips 1994, Montgomery & Craig 2005, Booth 2011). CH: Cape Howe; NC: North Cape

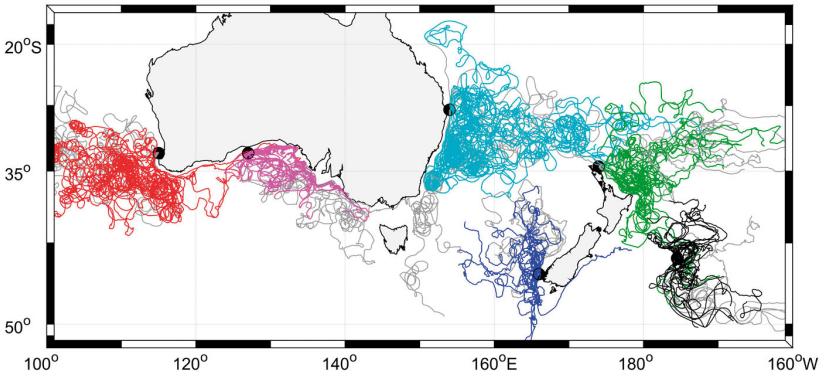

Fig. 4. Simulated trajectories for larvae released at 6 representative hatching locations (Fig. 1). For each hatching location (black dots), simulated larvae were released on 1 October each year from 1993 to 2008 in the Bran 3.5 hindcast (see 'Methods') and allowed to disperse for 3 yr. There are 16 trajectories for each hatching location. The first 18 mo of each trajectory is shown in colour, with the remaining 18 mo shown in grey

RESULTS

Generalised simulation

To illustrate the single-particle Lagrangian method and give a qualitative sense of the likely larval dispersal for different regions, Fig. 4 shows trajectories of simulated larvae released on 1 October in each of the 16 yr from 6 representative hatching locations. The full analyses contains 192 trajectories from each location, but for clarity we plot only these 16 trajectories.

For larvae released off WA near the southern limit of *Panulirus cygnus* populations, most (13) trajectories remain in the Indian Ocean, although some larvae head north against the mean direction of the Leeuwin current. A small number of larvae (3) become entrained in the South Australia Current, and 2 of these then return in the

offshore Flinders Current. For larvae released off South Australia near the western limit of *Jasus edwardsii* populations, all larvae initially flow eastwards in the South Australia Current, but then get entrained in recirculation between this current and the Flinders Current, so that most larvae remain in the Great Australian Bight. Almost all larvae released off Queensland at about the northern limit of *Sagmariasus verreauxi* populations enter the East Australian Current and then become entrained in the eddy system associated with recirculation within the East Australian Current and the Tasman Front, although one larva flows to north of 20°S before recirculating to the south.

Larvae released off North Cape, New Zealand, mostly become entrained in the East Auckland Current (10 larvae). Some then disperse to the northeast of New Zealand following the recirculation of the East Auckland Current (e.g. Chiswell et al. 2015). However, a substantial fraction (6) become entrained in East Cape Current and then the Wairarapa Eddy. A smaller proportion (2) flows to the south and becomes entrained in the Subtropical Front. Larvae released off the southwest of the South Island tend to remain in the southern Tasman Sea, with some getting about halfway to Australia within 18 mo. One larva becomes entrained in the Southland Current flowing up the east coast of the South Island. Larvae released off the Chatham Islands are retained mainly east of the islands, although a substantial fraction (5 of 16) larvae head north to become entrained in the eddy system east of the North Island.

Spatial kernels of settlement as a function of PLD

The generalised simulation allows us to investigate the spatial kernels of settlement as a function of PLD (Fig. 5). For each PLD, we show the settlement

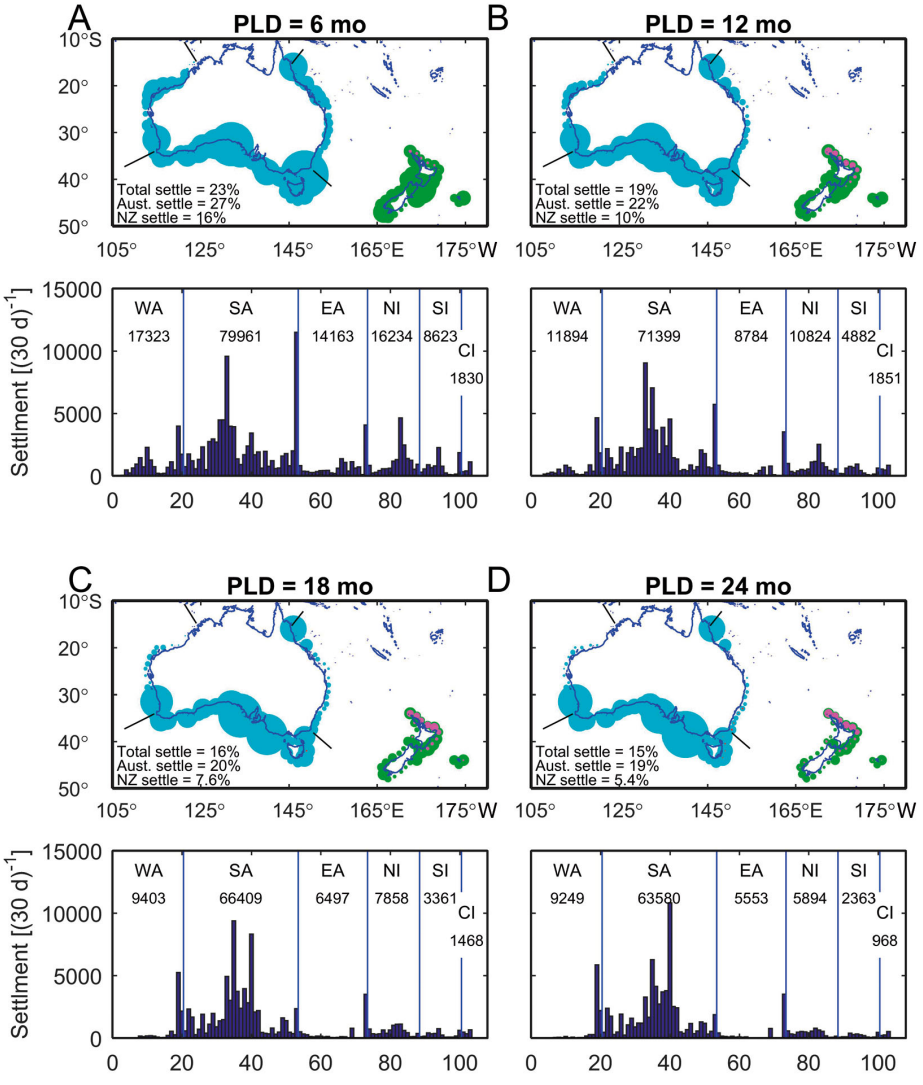

Fig. 5. Spatial kernels of simulated settlement for larvae released 1 October every year from 1993 to 2008 at the 103 hatching locations shown in Fig. 1. Settlement is shown for various pelagic larval durations (PLD). (A) PLD = 6 mo; (B) PLD = 12 mo; (C) PLD = 18 mo; (D) PLD = 24 mo. Larvae are assumed to be able to metamorphose and settle if they are within 100 km of the coast during a 30 d competency period centred on each PLD. The simulated settlement is the number of larvae that settle during this 30 d competency period and has units of settlers per 30 d. Upper panels show the settlement location; cyan signifies settlement in Australia from Australian hatching, green signifies settlement in New Zealand from New Zealand hatching, magenta signifies settlement in New Zealand from Australian hatching. Lower panels: histograms of the settlement binned into the 103 locations shown in Fig. 1. Numbers indicate total number of settlers (per 30 d) by region

geographically (upper panel) and binned by location index (lower panel).

There are 19776 trajectories in the generalised simulation (103 locations × 192 trajectories location^{-1}). The settlement algorithm allows settlement over a 30 d competency period, so the maximum possible settlement for any given PLD (which would occur if all simulated larvae remained within 100 km of the coast during the entire 30 d period) is 593280 settlers.

For a 6 mo PLD, there are 139057 settlers, which is about 23% of the maximum settlement. Of these, about 111000 settle in Australia and about 28000 settle in New Zealand. Every larva settles in the same country in which it was hatched, and the settlement rate is about 27% for Australia and about 16% for New Zealand. Thus, for 6 mo PLD, the settlement rate for Australia is about 70% higher than for New Zealand. As the PLD increases, the settlement rates in Australia and New Zealand behave quite differently, with the settlement rate in Australia steadying to about 20% for PLDs greater than 9 mo, whereas the settlement rate in New Zealand progressively declines to reach 5% for a PLD of 24 mo.

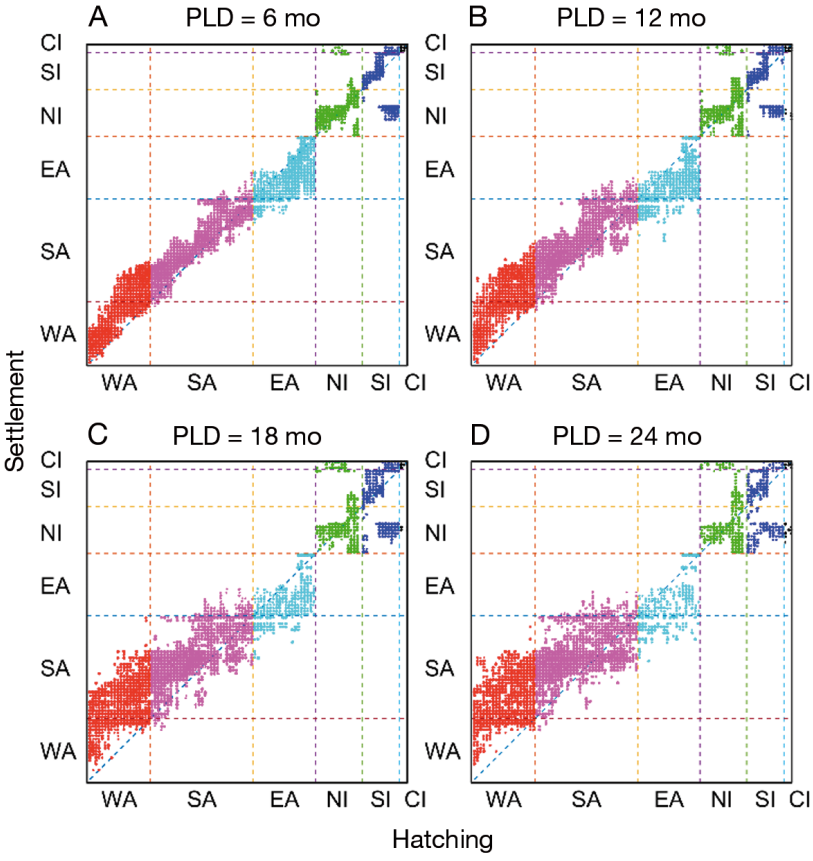

Fig. 6. Settlement versus hatching region for simulations made with the 103 potential hatching locations shown in Fig. 1 for various pelagic larval duration (PLD). (A) PLD = 6 mo; (B) PLD = 12 mo; (C) PLD = 18 mo; (D) PLD = 24 mo. The plot has been colour coded according to hatching region (Fig. 1). For example, red dots indicate larvae that were hatched in WA. The $x = y$ line indicates larvae settle where they hatch; points above the line indicate settlement generally to the south of hatching for WA, to the east for SA, to the north for EA, and to the south for New Zealand

Settlement is not spatially uniform around the coast of either country, and the spatial kernels change as the PLD increases. As expected, settlement tends to occur downstream of hatching and this is perhaps most obvious on the east and west coasts of Australia, where larvae are advected to the north and south by the North Queensland, East Australian and Leeuwin Currents. As the PLD increases, settlement in Australia tends to become more focussed around SA, so that for PLDs longer than 12 mo, there is very little settlement outside of SA. Settlement in New Zealand tends to be highest along the east coast of the North Island and west coast of the South Island (Fig. 5).

The geographic distribution of settlement as a function of PLD can also be visualised by plotting the settlement location as a function of hatching location (Fig. 6). For a PLD of 6 mo, most settlement is within the hatching region, except that much of the hatching in WA settles in SA and some settlement from SI occurs from hatching in NI. As the PLD lengthens, there is more settlement downstream for each hatching location. For example, for an 18 mo PLD, the majority of larvae hatched in WA settle in SA, and in New Zealand, much of the SI hatching settles in NI.

Mean temperature experienced by larvae during dispersal

The distribution of MTD, along with its upper and lower 5th percentiles, is plotted as a function of settlement location for various PLD in Fig. 7. We also show the local mean ocean temperature at each settlement location (which would be the MTD if larvae spent their entire pelagic phase at the settlement location).

Regardless of PLD, the peak in MTD distribution over most of the domain is about the same as the

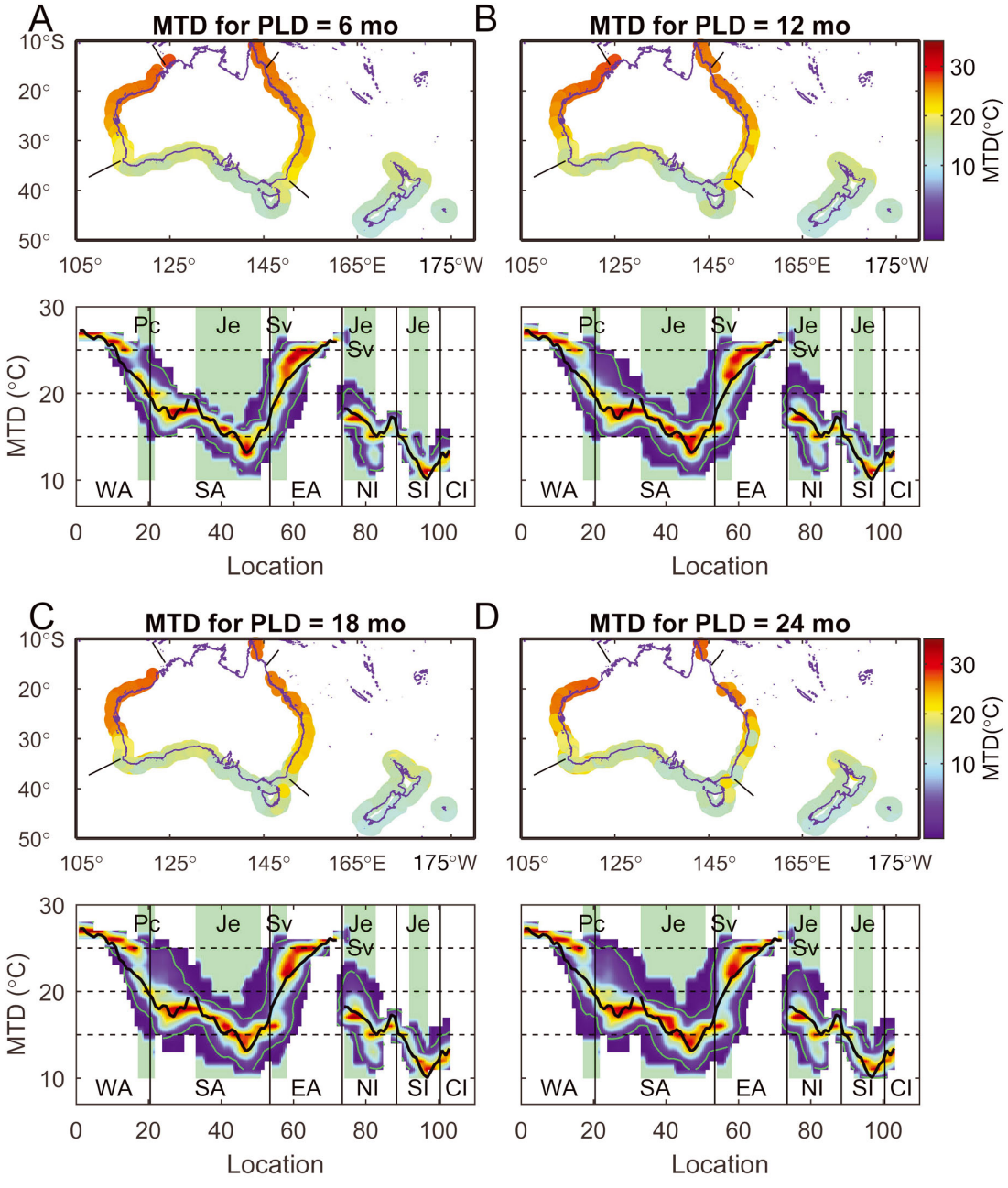

Fig. 7. Mean temperature experienced by larvae during their pelagic phase (MTD) for various pelagic larval durations (PLD). (A) PLD = 6 mo; (B) PLD = 12 mo; (C) PLD = 18 mo; (D) PLD = 24 mo. Upper panels: MTD at simulated settlement locations. Geographic regions (WA, SA, EA, NI, SI, and CI) are as shown in Fig. 1. Lower panels: distribution of MTD as a function of location index (see Fig. 1). Green lines: upper and lower 5th percentiles of the distribution, used as an index of the range in MTD; black line: mean ocean temperature at the coast. Green vertical shading: observed settlement regions for the 3 species — *Panulirus cygnus* (Pc) settles mostly in WA, *Jasus edwardsii* (Je) settles in SA, NI and SI, *Sagmariasus verreauxi* (Sv) settles in EA and NI

mean local temperature. However, in central WA north of the Abrolhos Islands (Fig. 1, location 16) and along most of the east coast of Australia, MTD is warmer than the local temperature by as much as 3°C. As the PLD increases, the peak in MTD does not change appreciably. However, the range increases, so that for a PLD of 24 mo, the MTD range across SA is about 50% higher than for a PLD of 6 mo.

Thus, MTD is not substantially different from the local ocean temperature at settlement where the local currents are largely zonal and there is little long-current temperature gradient. MTD tends to be

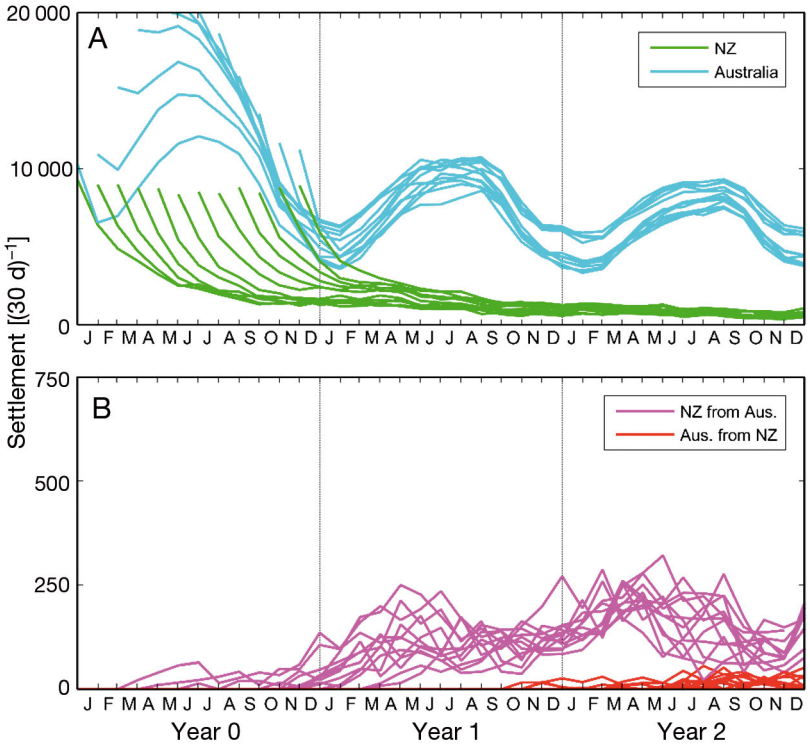

Fig. 8. Potential settlement as a function of pelagic larval duration (PLD) for the generalised simulation where simulated larvae were released at all 103 hatching locations shown in Fig. 1. For each date, potential settlement was computed as the number of larvae that were within 100 km of the coast during a 30 d competency period centred on that date, and has units of settlers per 30 d. Simulations were made for hatching on the first day of each month (January to December; see 'Methods'). (A) Settlement in Australia from Australian hatching (cyan) and settlement in New Zealand from New Zealand hatching (green), (B) Settlement in New Zealand from Australian hatching (magenta) and settlement in Australia from New Zealand hatching (red). Note the difference in scale between (A) and (B)

warmer than the local ocean along the west and east coasts where the local currents (Leeuwin and East Australian Currents, respectively) are meridional and there is a large along-current temperature gradient.

Temporal kernels of settlement

To illustrate how settlement varies in time for each country, the settlement averaged over all 16 yr is plotted as a function of time for each hatching month in Fig. 8.

Regardless of the month in which the larvae hatched, settlement around Australia from Australian sources shows a strong annual cycle, with a broad winter peak (June to September) that is nearly double the preceding summer minimum (January and February). After the hatching year there is about a 20% reduction in settlement yr^{-1}. In contrast, regardless of hatching month, settlement in New Zealand from New Zealand sources decreases with time.

Settlement can occur in each country from hatching in the other country as a result of trans-Tasman dispersal, although at very low levels (note the change in scale between Fig. 8A and B). Settlement in New Zealand from Australian sources increases for about 2 yr after hatching (reflecting the length of time it takes larvae to cross the Tasman Sea) before decreasing. Settlement in Australia from New Zealand sources occurs at very low levels 1 yr or more after hatching.

Species-specific simulations

The species-specific simulations were made by selecting trajectories that originated at the locations corresponding to the adult populations (Figs. 2 & 3) and started in the hatching months appropriate for each species. The results are presented for PLDs spanning the presumed PLD of each species (Table 1).

Spatial kernels

Fig. 9 shows spatial kernels of settlement for *P. cygnus* for PLDs of 9, 12 and 18 mo. Here, hatching was in January with adult/hatching populations in WA (Fig. 3). Simulated settlement occurs in 2 geographical areas. Settlement near the WA–SA border reasonably well overlaps the observed settlement (Fig. 3). However, the model also suggests significant settlement in SA that has not been documented in reality. For a PLD of 9 mo (the lower end of the observed PLD), we obtain 166 settlers in the bins corresponding to the observed settlement, which represents about 0.3% of the total potential settlement, i.e. 0.3% of all simulated larvae hatched at *P. cygnus* adult locations settle for this PLD. This settlement rate increases slightly for a PLD of 12 mo, but then decreases for longer PLDs.

Fig. 10 shows spatial kernels for *J. edwardsii* for PLDs of 15, 21 and 27 mo. Here, hatching was in October with adult populations in SA, NI, SI and CI as shown in Fig. 2. Australian settlement is densest in

Table 1. Hatching and settlement times and pelagic larval duration (PLD) for lobster species

	Hatching	Peak Settlement	PLD (months)	Reference
Jasus caveorum Webber & Booth, 1995	?	?	?	
Jasus edwardsii (Hutton, 1875)	Sep–Nov	Jun–Jul	12–≥24	Booth (2006), Chiswell & Booth (2008), Linnane et al. (2010), Bradford et al. (2015)
Jasus frontalis (H. Milne Edwards, 1837)	Austral spring/ summer	?	12	Arana et al. (1985), Dupré (2003), Porobi et al. (2013)
Jasus lalandii (H. Milne Edwards, 1837)	Sep–Nov	Dec–Apr	9–10, 14–18	Pollock (1986), George (2005)
Jasus paulensis (Heller 1862)	Austral spring	?	?	Grua (1960)
Jasus tristani Holthuis, 1963	Austral spring/ summer	?	9 (?)	Heydorn (1969), Roscoe (1979), Lutjeharms & Heydorn (1981)
Panulirus cygnus George, 1962	Nov–Feb	Sep–Jan	9–12	Griffin et al. (2001), de Lestang et al. (2012)
Sagmariasus verreauxi (H. Milne Edwards, 1851)	Dec–Jan	Sep–Jan	8–12	Montgomery & Craig (2005), Booth (2011)

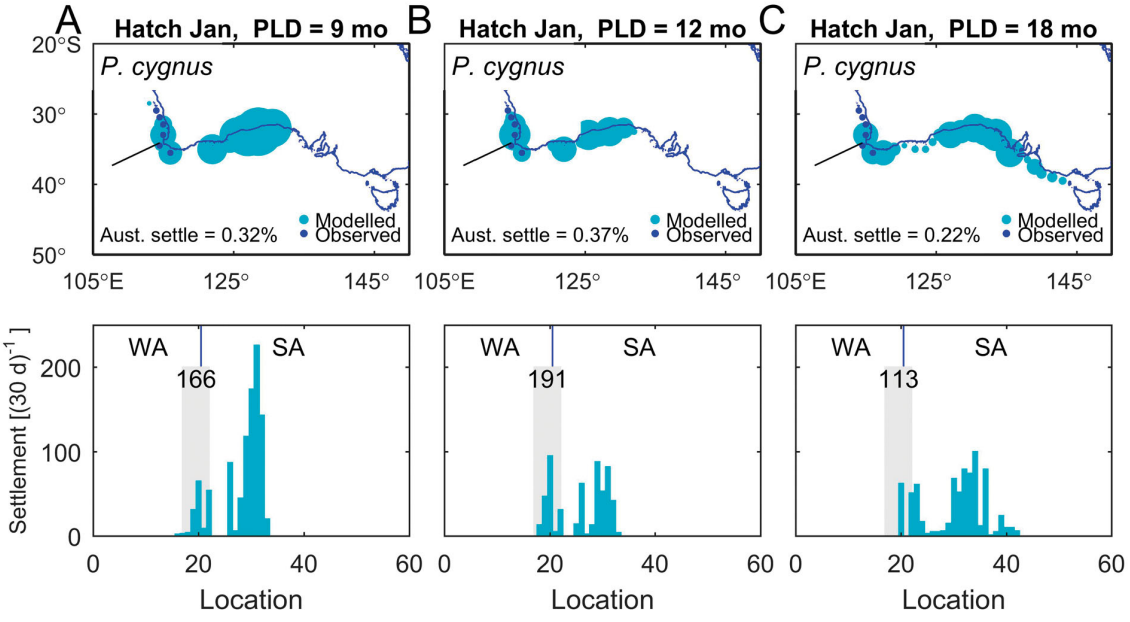

Fig. 9. Simulated settlement of *Panulirus cygnus* for various pelagic larval durations (PLD). (A) PLD = 9 mo; (B) PLD = 12 mo; (C) PLD = 18 mo. Single-particle Lagrangian simulations were made assuming the larvae were hatched on 1 January every year between 1993 and 2008 at the *P. cygnus* adult locations shown in Fig. 3A. Upper panels show the settlement location with cyan signifying simulated settlement in Australia from Australian hatching. Blue dots: observed settlement locations shown in Fig. 3A. Lower panels show histograms of the settlement (settlers per 30 d) binned into the 103 locations shown in Fig. 1. Shaded areas: observed *P. cygnus* settlement locations shown in Fig. 3A; numbers: total number of simulated settlers during the competency period by region

eastern SA and almost exactly matches the observed distribution, although there is some settlement at very low levels in EA. For a PLD of 15 mo, we obtain 1406 settlers in the region corresponding to observed settlement, which represents about 3% of the total potential settlement. The rate nearly doubles for PLD of 21 mo, but returns to about 3% for a PLD of 27 mo. New Zealand settlement shows highest settlement in the east coast of the North Island and southwest coast of the South Island, also consistent with observations, except that the model does not produce settlement in the north of the North Island. Settlement rates are considerably lower than for Australia with settlement rates decreasing monotonically from 0.8 to 0.3%.

Fig. 11 shows spatial kernels for *S. verreauxi* for PLDs of 9, 12 and 18 months. Here, hatching was in December with adult populations in EA and NI as shown in Fig. 3. Simulated settlement is much lower for this species than the others, so that there is much higher uncertainty about the results. Nevertheless, in

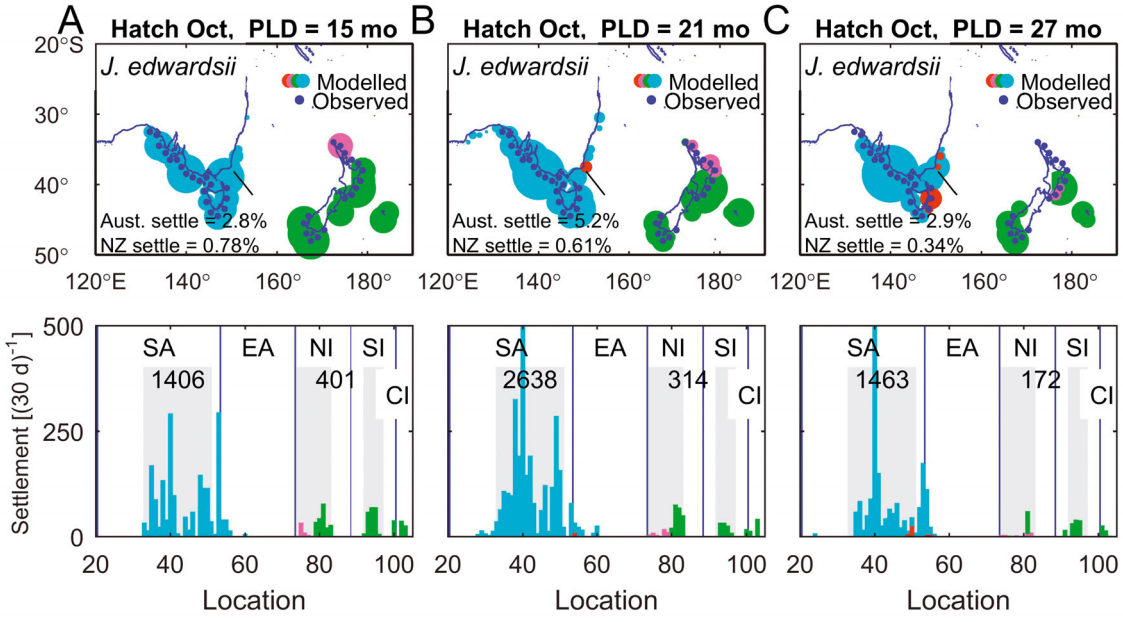

Fig. 10. Simulated settlement of *Jasus edwardsii* for various pelagic larval durations (PLD). (A) PLD = 15 mo; (B) PLD = 21 mo; (C) PLD = 27 mo. Single-particle Lagrangian simulations were made assuming the larvae were hatched on 1 October every year between 1993 and 2008 at the *J. edwardsii* adult locations shown in Fig. 2. Upper panels show the settlement location with cyan signifying settlement in Australia from Australian hatching, red signifying settlement in Australia from New Zealand hatching, green signifying settlement in New Zealand from New Zealand hatching, and magenta signifying settlement in New Zealand from Australian hatching. Blue dots: observed settlement locations shown in Fig. 2. Lower panels show histograms of the settlement (settlers per 30 d) binned into the 103 locations shown in Fig. 1. Shaded areas: observed *J. edwardsii* settlement locations shown in Fig. 2; numbers: total number of settlers during the competency period by region

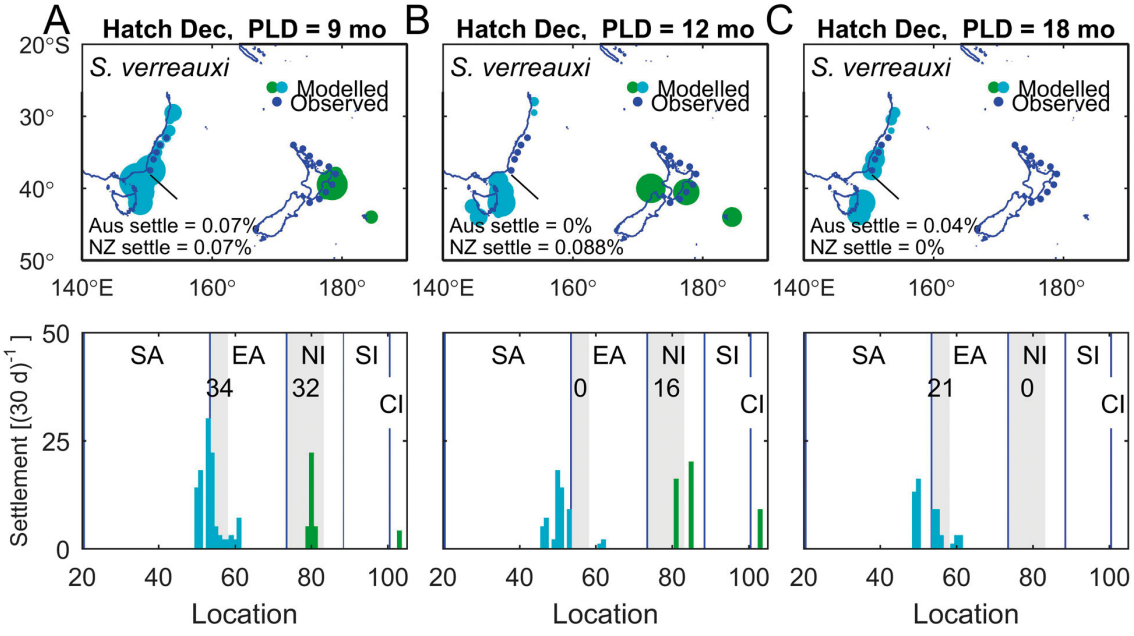

Fig. 11. Simulated settlement of *Sagmariasus verreauxi* for various pelagic larval durations (PLD). (A) PLD = 9 mo; (B) PLD = 12 mo; (C) PLD = 18 mo. Single-particle Lagrangian simulations were made assuming the larvae were hatched on 1 January every year between 1993 and 2008 at the *S. verreauxi* adult locations shown in Fig. 3B,C. Upper panels show the settlement location with cyan signifying simulated settlement in Australia from Australian hatching and green signifying settlement in New Zealand from New Zealand hatching. Blue dots: observed settlement locations shown in Fig. 3B,C. Lower panels show histograms of the settlement (settlers per 30 d) binned into the 103 locations shown in Fig. 1. Shaded areas: observed *S. verreauxi* settlement locations shown in Fig. 3B,C; numbers: total number of simulated settlers during the competency period by region

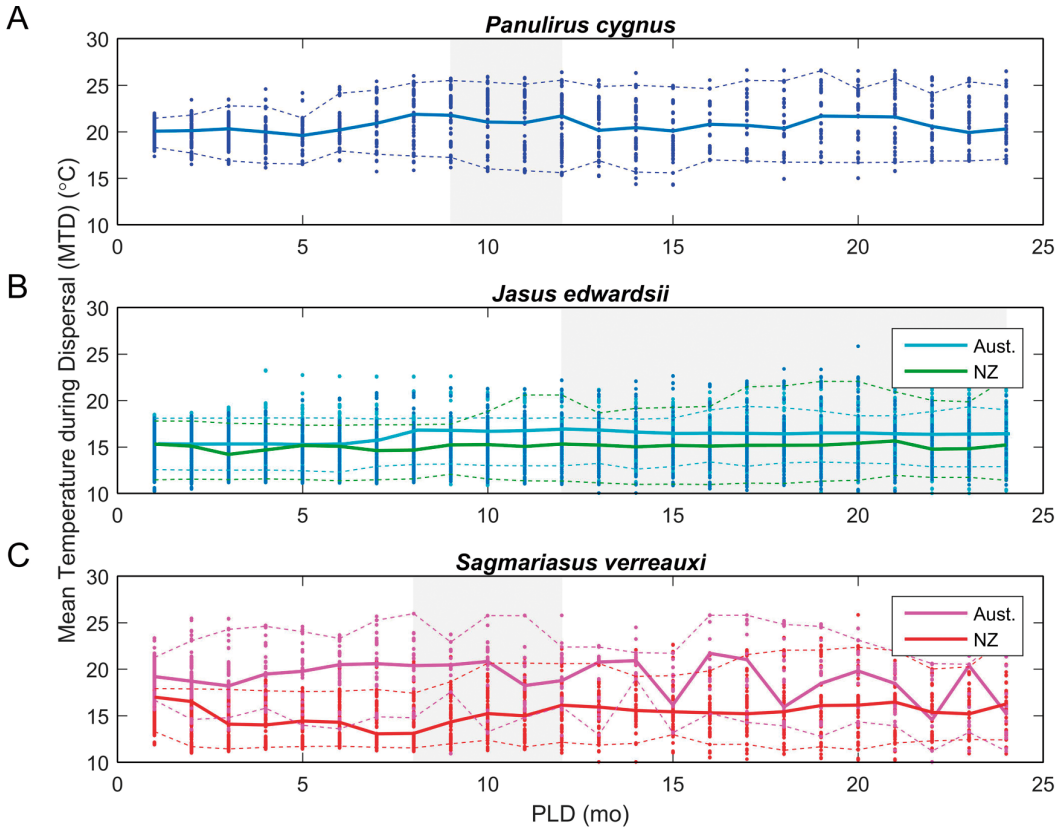

Fig. 12. Mean temperature experienced by simulated larvae during their pelagic phase (MTD) plotted as a function of pelagic larval duration (PLD) for 3 species of lobster: (A) *Panulirus cygnus*, (B) *Jasus edwardsii*, and (C) *Sagmariasus verreauxi*. Dots indicate the range in MTD, and for each species, the median MTD is indicated by the solid lines, dashed lines indicate the upper and lower 5th percentiles. For *J. edwardsii* and *S. verreauxi* the points are colour coded by the country of settlement. Grey shaded areas indicate the presumed PLD estimates in the literature (see Table 1)

both countries most settlement is downstream of the adult populations due to the respective boundary currents. For a PLD of 9 mo, simulated settlement in both countries tends to overlap the observed locations, although there is relatively high settlement around Bass Strait and Tasmania in Australia (there is episodic settlement in this region; Montgomery & Craig 2005). For a PLD of 12 mo or more, we obtain such low levels of settlement that it becomes difficult to make any valid statement about the distributions.

Mean temperature during dispersal

The species-specific simulations allow us to compute the MTD for larvae that settle in regions of observed settlement. This MTD can be plotted as a function of PLD for each species (Fig. 12).

For *P. cygnus*, the median MTD across the observed settlement locations is 20 to 22°C, and the range between the upper and lower 5th percentiles is 10°C. There is a small annual cycle in MTD with a range of about 2°C, which may be due to annual cycles in the Leeuwin Current. For *J. edwardsii*, MTD is about 16.5°C for settlement in Australia, and about 15.5°C for settlement in New Zealand. The range in MTD is 6°C for Australia and 10°C for New Zealand populations. MTD for *S. verreauxi* shows more variability than for the other species, especially for PLD longer than 1 yr, reflecting the low settlement rates of this species in the model. However, it appears that MTD for Australian settlement is significantly higher (median ~21°C) than for New Zealand settlement (~15°C), with the range being ~10°C for both countries.

Temporal kernels

The simulated settlement as a function of time (i.e. the temporal kernels) for species-specific simulations is shown in Fig. 13. Also plotted is the observed settlement in each country where available.

As might be expected from the generalised simulation, simulated settlement in Australia for both *P.*

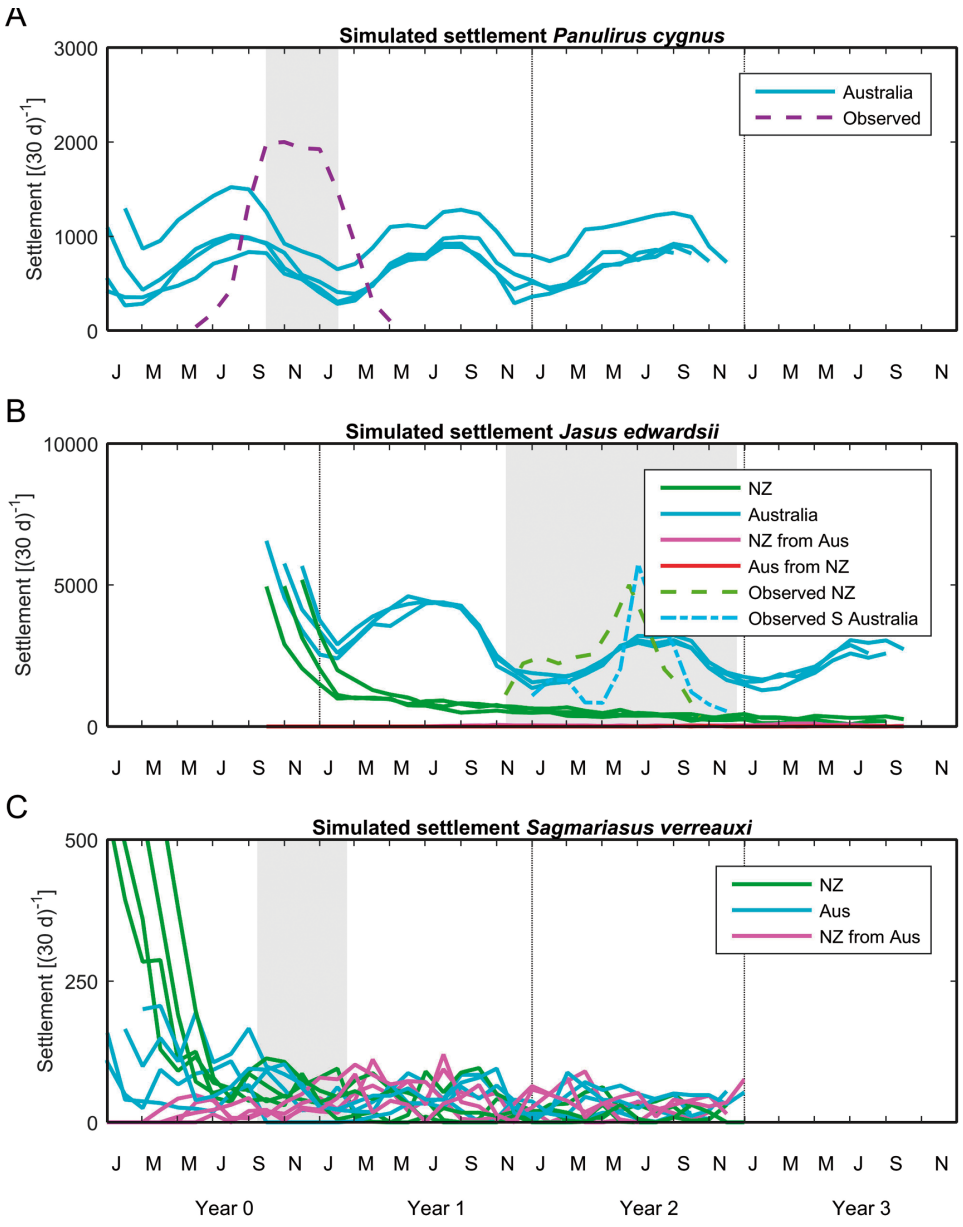

Fig. 13. Simulated settlement for the 3 lobster species (A) *Panulirus cygnus*, (B) *Jasus edwardsii*, and (C) *Sagmariasus verreauxi* as a function of time, where hatching occurs in Year 0. As in Fig. 8, for each date, settlement was computed as the number of simulated larvae that were within 100 km of the coast during a 30 d competency period centred on that date, and has units of settlers per 30 d. Dashed line in (A): mean *P. cygnus* settlement observed in Western Australia (de Lestang et al. 2012); dashed lines in (B): observed *J. edwardsii* settlement from New Zealand (Chiswell & Booth 2008) and averages of Blackfellows Caves, Beachport and Livingstons Bay, South Australia (Linnane et al. 2010, their Fig. 3). Observed settlement levels were rescaled by an arbitrary scaling factor. Grey areas: pelagic larval duration (PLD) estimates in the literature (see Table 1)

cygnus and *J. edwardsii* shows strong annual cycles with peak settlement in late winter, although settlement of *P. cygnus* is delayed compared to that of *J. edwardsii* by 2 to 4 mo. Observed settlement of *P. cygnus* takes place in spring–summer, with the observed settlement starting at about the time of maximum simulated settlement, but then continues as the simulated settlement drops off.

For *J. edwardsii*, however, there is remarkably good agreement in the timing between simulated and observed settlement in Australia, although the observations show a bimodal structure with a local maximum in summer (February) at about the time of the minimum in the simulated settlement. Simulated settlement in New Zealand decreases monotonically, also as expected from the generalised simulation.

Observed settlement in New Zealand has about the same timing as in Australia and also shows a local maximum in summer, although the bimodal nature is not as pronounced as in Australia.

Simulated settlement of *S. verreauxi* shows very low levels compared to that of *J. edwardsii* (note the different scales). This low level of settlement means that we cannot have any confidence in the temporal kernels, however, there is a slight suggestion of an annual cycle in settlement within Australia with higher levels in spring and early summer (September to November).

DISCUSSION

The generalised simulation was designed to investigate questions such as whether there are regions where ocean circulation alone leads to a particular PLD being favoured. Its results are principally that because of the boundary currents, settlement occurs downstream of hatching — especially on the west and east coasts of Australia, and that settlement in Australia has a strong annual cycle whereas settlement in New Zealand decreases monotonically with time. In addition, the mean ocean temperature during dispersal experienced by larvae depends on latitude but shows strong breaks around Cape Leeuwin in the west and Cape Howe in the east.

Many of these results are intuitively obvious, especially that where boundary currents are strong, local settlement drops rapidly as PLD increases; for example, the settlement rate within EA for a 12 mo PLD is about half the rate for a 6 mo PLD (Fig. 5). It should be noted that this does not necessarily imply that the ocean circulation leads to selection for shorter PLDs in these regions, because viable populations could be maintained with contranatant migration of juveniles.

The species-specific simulations were designed to model present-day larval dispersal for the 3 species of interest. However, we did not use hatching that accurately reflects true egg production rates in time or along the coast. Nor did we model such factors as spatially or temporally variable mortality of the larvae, or contranatant migration of juveniles. These factors were not included because we have a far from clear understanding of the geographical extent of larval production, behaviour of juveniles, or of the complex trophic interactions between phyllosomas and their predators and prey. As a result, some care must be taken in interpreting the results. In particular, we cannot estimate with any accuracy the proportion of settlement in New Zealand that originates in Australia. Nevertheless, the species-specific simulations can be used to infer some information about behaviour of the respective adults or larvae.

The case of *Panulirus cygnus* (Fig. 9) is a good example of where settlement is strongly displaced downstream of hatching by the local boundary current. This role of the boundary current is supported by the well documented contranatant migration of juveniles, and by observations that when the Leeuwin Current is stronger (generally in La Niña years; Feng et al. 2003), observed settlement in the region is displaced more to the south (Caputi et al. 2001). Simulated settlement of *P. cygnus* shows high levels in SA but we are not aware of any settlement having been observed there. Why this should be is open to speculation. The break in MTD about Cape Leeuwin (Fig. 7) raises the possibility that *P. cygnus* phyllosomas do not survive MTD less than about 23°C, but this is not supported by laboratory measurements where Liddy et al. (2004) found survival of *P. cygnus* phyllosomas did not significantly differ at any of 3 temperatures (19, 22 or 25°C). It may be, as speculated by Griffin et al. (2001), that prey levels in the Great Australian Bight are too low, or predation is too high for *P. cygnus* phyllosomas to survive long there. An alternative reason, suggested by a reviewer, is given by Feng et al. (2011), who modelled *P. cygnus* recruitment with and without Stokes drift. They found that by including Stokes drift, they were able to overcome a problem with a previous model (Griffin et al. 2001) that also found too much settlement along the south coast. However, no matter what the reason for the discrepancy, the presumed low observed settlement in the Great Australian Bight suggests that for *P. cygnus*, only settlement north of Cape Leeuwin leads to recruitment to the adult populations. If so, there is little advantage to having a long PLD.

For *Sagmariasus verreauxi*, simulated settlement in Australia spans observed settlement locations in EA, but also occurs around Tasmania where there is only episodic observed settlement (Montgomery & Craig 2005). MTD around Tasmania is typically about 10 to 12°C regardless of PLD. As with *P. cygnus*, this suggests that *S. verreauxi* phyllosomas may not survive the cooler waters to the south, and in this case, this idea is supported by laboratory cultures which suggest that optimal growths occur at about 23°C, with growth at 17°C occurring at substantially lower rates (Fitzgibbon & Battaglene 2012). Simulated settlement of *S. verreauxi* in New Zealand occurs at very low levels, only for PLDs of 9 and 12 mo, and only over part of the observed settlement range.

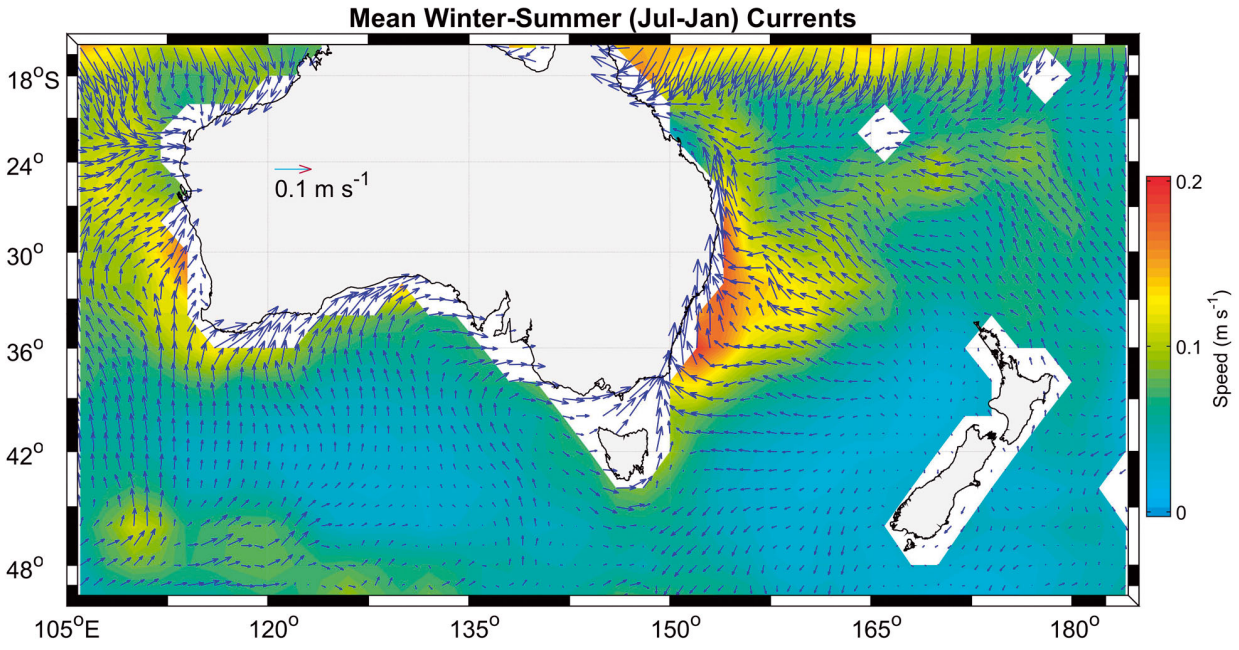

Fig. 14. Difference between weighted mean currents in winter (July) and summer (January) from 19 yr of Bran 3.5 hindcast. The weighting is 2/3 times the surface current plus 1/3 times the 100 m current (see 'Methods')

Median MTD for *S. verreauxi* settlement in New Zealand is ~15°C, although the upper 5th percentile is close to 20°C. If the laboratory results of Fitzgibbon & Battaglene (2012) apply to the ocean, this would suggest there is high mortality around New Zealand due to cool ocean temperatures (although clearly enough phyllosomas survive to maintain the populations). The *S. verreauxi*-specific simulation has very low settlement and consequently high uncertainty in the results. However, it does suggest a picture that the geographical range of *S. verreauxi* in both Australia and New Zealand is determined by ocean temperatures.

The most non-intuitive findings of this work are the strong annual cycles in settlement around western and southern Australia seen in both the generalised and *Jasus edwardsii*-specific simulations (Figs. 8 & 13). This raises the question of whether these annual cycles lead to selection for long PLD. In the absence of other influences, there are likely to be more larvae within the 100 km settlement zone during winter than during summer by a factor of nearly 2. This should favour strong selection for long PLD because phyllosomas that delay their metamorphosis until winter will have a clear advantage over those that do not.

Fig. 13 shows encouragingly good agreement between the timing of the simulated and observed settlement in Australia. But it is worth noting that the winter peak in observed settlement could reflect an oceanic mechanism for increased retention rather than the true distribution of *J. edwardsii* PLD, and the settlement in New Zealand may be a better indicator of the true distribution of PLD.

Thus, we argue that the results shown in Fig. 13 are consistent with *J. edwardsii* selecting for ~20 mo PLD based on increased potential settlement in winter. The most obvious question is what is the ocean mechanism that leads to increased potential settlement in winter? Fig. 14 shows the difference between the mean summer (January) and mean winter (July) weighted surface/deep currents in Bran 3.5. Stronger onshore currents occur almost everywhere in winter around Australia, but not New Zealand. This increased onshore flow in winter is most likely an expression of stronger Ekman flow caused by stronger Trade winds in the north and stronger westerly winds in the south in winter (e.g. Hellerman & Rosenstein 1983).

Our simulations suggest that selection for long PLD of *J. edwardsii* may be driven by ocean circulation around Australia, but not around New Zealand. If so, then the long PLD in New Zealand populations suggests there is sufficient gene flow across the Tasman Sea to maintain homogeneity of the species. This is consistent with the lack of genetic differentiation between the 2 populations (Ovenden et al. 1997), and simulations of trans-Tasman larval dispersion by Chiswell et al. (2003), who suggest that there is some larval transport from Australia to New Zealand but very little in the opposite direction.

Our simulations do not preclude the hypothesis that the long *J. edwardsii* PLD evolved because its larvae experience cool ocean temperatures, and we would be better placed to exclude this hypothesis if we could show that other *Jasus* species have evolved shorter PLDs in equivalently cool ocean environments. Unfortunately, robust estimates of PLD for the other species are lacking, and as yet we have no models of MTD for these other species. However, *J. lalandii* is found predominantly on the west coast of southern Africa from Walvis Bay, Namibia to East London, South Africa (Van Zyl et al. 2003 and references therein) where upwelling reduces the mean ocean temperature to typically 15 to 17°C (Lutjeharms & Meeuwis 1987). Thus, *J. lalandii* is a cool-water species more equivalent to *J. edwardsii* than *P. cygnus* or *S. verreauxi*, yet published estimates of its PLD (ranging from 9–10 to 14–18 mo; Pollock 1986, George 2005) are shorter than those of *J. edwardsii.* Similarly, *J. frontalis* is found on Juan Fernandez and Desventuradas Islands where mean surface ocean temperatures are 16.8 and 18.8°C, respectively, which are comparable to the MTD for *J. edwardsii*, yet *J. frontalis* PLD may be as short as 12 mo (Porobi et al. 2013). While not conclusive, these observations tend to support the idea that there is no physiological or metabolic barrier that prevents *Jasus* species from evolving a PLD shorter than seen in *J. edwardsii* in cooler oceans, and so lends some support for our second hypothesis.

It is worthwhile noting, as a reviewer of this article commented, that the long PLD of *J. edwardsii* may be an ancestral feature that has not been eliminated, whereas long PLD for other *Jasus* species has been eliminated because they tend to be island species. It could be that long PLD may not be advantageous or particularly adaptive for *J. edwardsii*, and that the increased settlement in winter offsets the disadvantages of long PLD (rather than selects for it), so that having a long PLD may not be so bad that it is deleterious.

It is also possible that the entire *Jasus* genus may have a highly plastic PLD and that the long observed PLD for *J. edwardsii* is a physiological or metabolic response to the cooler ocean temperatures rather than an evolutionary response. Indeed, *J. edwardsii* appears to have a far greater capacity in nature to delay metamorphosis for long periods (months, possibly even years) than any other palinurid through mark-time moulting (Booth & Phillips 1994).

The main conclusion of this work is that while we cannot exclude the idea that the long PLD of *J. edwardsii* is an evolutionary response to relatively cool ocean temperatures, the indications are that closely-related species having much shorter PLD exist in equivalently cool environments. If so, it is likely that the long PLD of *J. edwardsii* is an evolutionary response to increased potential settlement in winter driven by stronger onshore Ekman flow. The idea that long larval life may be selected for as a response to ocean circulation is not new; for example, Pollock (1995), without discussing too much detail of potential mechanisms, suggested that long PLD and other life history adaptions of *Jasus* species evolved when the genus radiated in the late Miocene in response to the establishment of the Antarctic Circumpolar Current resulting from the opening of Drake Passage and the Tasmanian Gateway about 30 million years ago (Scher et al. 2015).

Thus, in summary, this work provides a possible explanation for the long PLD in *J. edwardsii*. Many of the conclusions presented here are speculative rather than definitive. The ambiguities might be eliminated in future models of the system that have a better understanding of the geographical extent and timing of hatching and settlement, of the metabolic requirements of phyllosoma, and of the predation and prey interactions that lead to spatially dependent mortality.

Acknowledgements. This work was funded by the New Zealand Government under a grant to the National Institute of Water & Atmospheric Research (NIWA). We thank P. Oke, D. Griffin, A. Schiller and CSIRO for access to the Bran 3.5 products. We thank NOAA for making the World Ocean Atlas data publically available. We also thank 3 anonymous reviewers whose comments helped substantially improve the article.

LITERATURE CITED

Annala JH, McKoy JL, Booth JD, Pike RB (1980) Size at the onset of sexual maturity in female *Jasus edwardsii* (Decapoda: Palinuridae) in New Zealand. N Z J Mar Freshw Res 14:217–227

Arana EP, Dupré M, Gaete MV (1985) Ciclo reproductivo, talla de primera madurez sexual y fecundidad de la langosta de Juan Fernandez (*Jasus frontalis*). In: Arana EP (ed) Investigaciones marinas en el Archipielago de Juan Fernandez. Universidad Catolica de Valparaiso, Valparaiso, p 187–211

Boland FM, Church JA (1981) The East Australian Current 1978. Deep-Sea Res A Oceanogr Res Pap 28:937–957

Booth JD (1994) *Jasus edwardsii* larval recruitment off the east coast of New Zealand. Crustaceana 66:295–317

Booth JD (1997) Long-distance movements in *Jasus* spp. and their role in larval recruitment. Bull Mar Sci 61:111–128

Booth JD (2002) Early life history, recruitment processes and settlement of spiny lobsters. Fish Sci 68:384–389

Booth JD (2006) *Jasus* species. In: Phillips BF (ed) Lobsters:

biology, management, aquaculture and fisheries. Blackwell Publishing, Oxford, p 340–358

Booth JD (2011) Spiny lobsters: through the eyes of the giant packhorse. Victoria University Press, Wellington

Booth JD, Phillips BF (1994) Early-life history of spiny lobster. Crustaceana 66:271–294

Bradford RW, Bruce BD, Chiswell SM, Booth JD, Jeffs A, Wotherspoon S (2005) Vertical distribution and diurnal migration patterns of *Jasus edwardsii* (Hutton, 1875) phyllosomas off the East Coast of the North Island, New Zealand. N Z J Mar Freshw Res 39:593–604

Bradford RW, Griffin D, Bruce BD (2015) Estimating the duration of the pelagic phyllosoma phase of the southern rock lobster, *Jasus edwardsii* (Hutton). Mar Freshw Res 66:213–219

Brown RS, Phillips BF (1994) The current status of Australia's rock lobster fisheries. In: Phillips BF, Cobb JS, Kittaka J (eds) Spiny lobster management. Blackwell Scientific Publications, Oxford, p 33–63

Butler MJ IV, Paris CB, Goldstein JS, Matsuda H, Cowen RK (2011) Behavior constrains the dispersal of long-lived spiny lobster larvae. Mar Ecol Prog Ser 422:223–237

Caputi N, Chubb C, Pearce A (2001) Environmental effects on recruitment of the western rock lobster, *Panulirus cygnus*. Mar Freshw Res 52:1167–1174

Chiswell SM (2013) Lagrangian time scales and eddy diffusivity at 1000 m compared to the surface in the South Pacific and Indian Oceans. J Phys Oceanogr 43:2718–2732

Chiswell SM, Booth JD (1999) Rock lobster *Jasus edwardsii* larval retention by the Wairarapa Eddy off New Zealand. Mar Ecol Prog Ser 183:227–240

Chiswell SM, Booth JD (2008) Sources and sinks of larval settlement in *Jasus edwardsii* around New Zealand: Where do larvae come from and where do they go? Mar Ecol Prog Ser 354:201–217

Chiswell SM, Rickard GJ (2008) Eulerian and Lagrangian statistics in the Bluelink numerical model and AVISO altimetry: validation of model eddy kinetics. J Geophys Res Oceans 113:C10024

Chiswell SM, Rickard GJ (2014) Evaluation of Bluelink hindcast BRAN 3.5 at surface and 1000m. Ocean Model 83:63–81

Chiswell SM, Wilkin J, Booth JD, Stanton B (2003) Trans-Tasman Sea larval transport: Is Australia a source for New Zealand rock lobsters? Mar Ecol Prog Ser 247:173–182

Chiswell SM, Bostock HC, Sutton PJH, Williams MJM (2015) Physical oceanography of the deep seas around New Zealand: a review. N Z J Mar Freshw Res 49: 286–317

de Lestang S, Caputi N (2015) Climate variability affecting the contranatant migration of *Panulirus cygnus*, the western rock lobster. Mar Biol 162:1889–1900

de Lestang SN, Caputi N, How J, Melville-Smith R, Thomson A, Stephenson P (2012) Stock assessment for the West Coast Rock Lobster fishery. Fisheries Res Rep No. 217, Department of Fisheries, North Beach

Dupré EM (2003) Reproductive and development of the Juan Fernandez spiny lobster, *Jasus frontalis* (H. Milne-Edwards, 1837). Minireview. Instituto de Ciencias del Mar y Limnología, UNAM. Contribuciones al Estudio de los Crustaceos del Pacifico Este 2:205–217 (in Spanish)

Fitzgibbon QP, Battaglene SC (2012) Effect of water temperature on the development and energetics of early, mid and late-stage phyllosoma larvae of spiny lobster *Sagmariasus verreauxi*. Aquaculture 344-349:153–160

Feng M, Meyers G, Pearce A, Wijffels S (2003) Annual and interannual variations of the Leeuwin Current at 32°S. J Geophys Res 108:3355

Feng M, Caputi N, Penn J, Slawinski D and others (2011) Ocean circulation, Stokes drift, and connectivity of western rock lobster (*Panulirus cygnus*) population. Can J Fish Aquat Sci 68:1182–1196

Fletcher W, Chubb C, McCrea J, Caputi N, Webster F, Gould R, Bray T (2005) Western rock lobster fishery. ESD Rep Ser No. 4. Department of Fisheries, Western Australian Fisheries and Marine Research Laboratories, North Beach

George RW (2005) Review: evolution of life cycles, including migration in spiny lobsters (Panlinuridae). N Z J Mar Freshw Res 39:503–514

Godfrey JS, Ridgway KR (1985) The large-scale environment of the poleward-flowing Leeuwin Current, Western-Australia: longshore steric height gradients, wind stresses and geostrophic flow. J Phys Oceanogr 15: 481–495

Griffin DA, Wilkin JL, Chubb CF, Pearce AF, Caputi N (2001) Ocean currents and the larval phase of Australian western rock lobster, *Panulirus cygnus*. Mar Freshw Res 52:1187–1199

Groeneveld JC, Von der Heyden S, Matthee CA (2012) High connectivity and lack of mtDNA differentiation among two previously recognized spiny lobster species in the southern Atlantic and Indian Oceans. Mar Biol Res 8: 764–770

Grua P (1960) Les langoustes australes (*Jasus paulensis*). Terres Australes et Antarctiques Francaises 10:14–40

Heath RA (1972) The Southland Current. N Z J Mar Freshw Res 6:497–533

Hellerman S, Rosenstein M (1983) Normal monthly wind stress over the world ocean with error estimates. J Phys Oceanogr 13:1093–1104

Heydorn AEF (1969) The South Atlantic rock lobster *Jasus tristani* at Vema Seamount, Gough Island and Tristan da Cunha Islands. Investigational Report 73, Sea Fisheries Branch, The Division, Cape Town

Hinojosa IA, Green BS, Gardner C, Hesse J, Stanley JA, Jeffs AG (2016) Reef sound as an orientation cue for shoreward migration by pueruli of the rock lobster, *Jasus edwardsii*. PLOS ONE 11:e0157862

Jeffs AG, Chiswell SM, Booth JD (2001) Distribution and condition of pueruli of the spiny lobster *Jasus edwardsii* offshore from north-east New Zealand. Mar Freshw Res 52:1211–1216

Jeffs AG, Montgomery JC, Tindle CT (2005) How do spiny lobster post-larvae find the coast? N Z J Mar Freshw Res 39:605–618

Kessler WS, Gourdeau L (2007) The annual cycle of circulation of the southwest subtropical Pacific, analyzed in an ocean GCM. J Phys Oceanogr 37:1610–1627

Liddy GC, Phillips BF, Maguire GB (2004) Effects of temperature and food density on the survival and growth of early stage phyllosoma of the western rock lobster, *Panulirus cygnus*. Aquaculture 242:207–215

Linnane A, James C, Middleton J, Hawthorne P, Hoare M (2010) Impact of wind stress anomalies on the seasonal pattern of southern rock lobster (*Jasus edwardsii*) settlement in South Australia. Fish Oceanogr 19:290–300

Locarnini RA, Mishonov AV, Antonov JI, Boyer TP and others (2010) World ocean atlas 2009, Vol 1: temperature. NOAA, Washington, DC

Lutjeharms JRE, Heydorn AEF (1981) The rock-lobster *Jasus tristani* on Vema Seamount: drifting buoys suggest a possible recruiting mechanism. Deep-Sea Res A, Oceanogr Res Pap 28:631–636

Lutjeharms JRE, Meeuwis JM (1987) The extent and variability of south-east Atlantic upwelling. S Afr J Mar Sci 5: 51–62

Middleton JF, Cirano M (2002) A northern boundary current along Australia's southern shelves: the Flinders Current. J Geophys Res 107:3129

Montgomery SS, Craig JR (2005) Distribution and abundance of recruits of the eastern rock lobster (*Jasus verreauxi*) along the coast of New South Wales, Australia. N Z J Mar Freshw Res 39:619–628

O'Connor MI, Bruno JF, Gaines SD, Halpern BS, Lester SE, Kinlan BP, Weiss JM (2007) Temperature control of larval dispersal and the implications for marine ecology, evolution, and conservation. Proc Natl Acad Sci USA 104: 1266–1271

Oke PR, Sakov P, Cahill ML, Dunn JR and others (2013) Towards a dynamically balanced eddy-resolving ocean reanalysis: BRAN3. Ocean Model 67:52–70

Oliphant A, Hauton C, Thatje S (2013) The implications of temperature-mediated plasticity in larval instar number for development within a marine invertebrate, the shrimp *Palaemonetes varians.* PLOS ONE 8:e75785

Ovenden JR, Booth JD, Smolenski AJ (1997) Mitochondrial DNA phylogeny of red and green rock lobsters (genus *Jasus*). Mar Freshw Res 48:1131–1136

Pollock DE (1986) Review of the fishery for and biology of the Cape rock lobster *Jasus lalandii* with notes on larval recruitment. Can J Fish Aquat Sci 43:2107–2117

Pollock DE (1995) Evolution of life-history patterns in three genera of spiny lobsters. Bull Mar Sci 57:516–526

Porobi J, Canales-Aguirre CB, Ernst B, Galleguillos R, Hernández CE (2013) Biogeography and historical demography of the Juan Fernández rock lobster, *Jasus frontalis* (Milne Edwards, 1837). J Hered 104:223–233

Roscoe MJ (1979) Biology and exploitation of the rock lobster *Jasus tristani* at the Tristan da Cunha Islands, South Atlantic, 1949-1976. Investigational Report No. 118, Sea Fisheries Branch, Cape Town

Siegel DA, Kinlan BP, Gaylord B, Gaines SD (2003) Lagrangian descriptions of marine larval dispersion. Mar Ecol Prog Ser 260:83–96

Stanton BR, Sutton PJH, Chiswell SM (1997) The East Auckland Current, 1994–95. N Z J Mar Freshw Res 31: 537–549

Van Zyl RF, Mayfield S, Branch GM (2003) Aquarium experiments comparing the feeding behaviour of rock lobster *Jasus lalandii* on abalone and sea urchins at two sites on the west coast of South Africa. Afr J Mar Sci 25:377–382

Editorial responsibility: Alejandro Gallego, Aberdeen, UK

Submitted: December 13, 2016; Accepted: June 21, 2017
Proofs received from author(s): July 28, 2017